RSC Advances

ROYAL SOCIETY OF CHEMISTRY

www.rsc.org/advances

DFT Studies on the Mechanism of Palladium catalyzed Arylthiolation of Unactive Arene to Diaryl Sulfide

Ya-ping Zhou, Mei-yan Wang, Sheng Fang, Yu Chen, Jing-yao Liu**

Institute of Theoretical Chemistry, Jilin University, Changchun 130023, People's Republic of China.

E-mail address: ljy121@jlu.edu.cn (J.L.); mywang858@163.com (M.W.)

Abstract: Palladium catalyzed arylthiolation of benzene with 1-(phenylthio) pyrrolidine-2,5-dione to form diaryl sulfide has been studied with the aid of density functional theory (DFT) calculations. Two catalytic cycles (I and II) were considered. In catalytic cycle I, the active species reacts first with benzene, while in catalytic cycle II, the active species reacts first with 1-(phenylthio) pyrrolidine-2,5-dione. The calculations show that catalytic cycle I is more favorable than catalytic cycle II. The reaction proceeds through C-H bond activation, concerted σ-bond metathesis, isomerization, ligand exchange, N-H protonation, and ligand exchange steps, where the concerted σ-bond metathesis is found to be the rate-determining step. The present mechanism slightly differs from the mechanism proposed by experiment, in which oxidative addition step rather than metathesis is involved. The frontier molecular orbitals were analyzed to understand the nature of different reaction mechanism between concerted σ-bond metathesis and oxidative addition. It is found that the HOMO-LUMO interaction results in concerted σ-bond metathesis, while the interaction between HOMO-1 and LUMO gives oxidative addition, and thus, the concerted σ-bond metathesis is more preferred in the arylthiolation reaction.

Keywords: Palladium catalyzed; Density functional theory; Arylthiolation; Arenes; Concerted σ-bond metathesis

1. Introduction

As the useful building blocks in organic synthesis,[1, 2] aryl sulfides widely exist in many high polymer material compounds and pharmaceutical molecules which are used for the treatment of diseases such as diabetes, Parkinson's disease, and HIV.[3-5] In the past decade years, transition metal catalyzed C-S coupling reactions of aryl halides with thiols has become one of the most powerful tools to form aryl sulfides.[6] The transition metals including palladium,[7, 8] copper,[9, 10] nickel,[11] iron,[12] and indium[13] have been exploited for C-S coupling reactions.[14] Considering the arenes or heteroarenes are cheaper and more available than aryl halides, transition metal catalyzed C-S coupling reaction via direct C-H bond activation has emerged as an attractive strategy for the synthesis of aryl sulfides.[15] Arylthiolation of C-H bonds of arenes[16-19] or heteroarenes[20-32] such as phenyl pyridine,[20-22] benzamide,[23-25] and benzothiazole[26, 27] has been widely investigated.

Generally, transition metal catalyzed arylthiolation of C-H bond suffers from harsh reaction conditions such as high temperature (80-140°C),[16, 17, 20-29, 31] and requirement of oxidizing agents.[16, 19-21, 27, 28] Although palladium catalyzed arylthiolation of arenes with p-tolunenesulfonyl cyanides can proceed at room temperature, low yield has been detected due to the formation of by-product diaryl sulfones.[18] Recently, Anbarasan *et al.* have reported that palladium catalyzed direct arylthiolation of unactivated arenes with (arylthio) pyrrolidine-2,5-diones can react under mild conditions (25°C), affording diaryl sulfides in high yield (eq 1).[33] A general plausible mechanism involving C-H activation, oxidative addition, and reductive elimination has been proposed by Anbarasan *et al.* (Scheme 1). While the σ-bond metathesis mechanism was found theoretically to be competitive with oxidative addition mechanism in several palladium catalyzed cross-coupling reactions,[34-36] it is interesting to figure out which mechanism oxidative addition or σ-bond metathesis is involved in the

arylthiolation reaction. Moreover, $Pd(TFA)_2$ (TFA= trifluoroacetate) was considered as the active species of catalyst in the proposed mechanism by Anbarasan *et al.*.[33] However, the formation of dicarboxylate-dicarboxylic acid palladium species $Pd(TFA)_2(HOAc)_2$ (HOAc = acetic acid) or $Pd(TFA)_2(HTFA)_2$ (HTFA = trifluoroacetic acid) has been proposed by Swang *et al.* with the aid of infrared spectroscopy when $Pd(OAc)_2$ (OAc = acetate) dissolved in HTFA.[37] Therefore, it is necessary to carry out theoretical calculations to determine the active species of catalyst and elucidate the detailed reaction mechanism for palladium catalyzed direct arylthiolation of arenes with 1-(arylthio) pyrrolidine-2,5-diones.

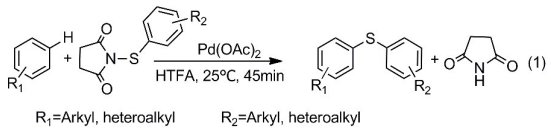

Please insert Scheme 1 here

In this paper, benzene and 1-(phenylthio) pyrrolidine-2,5-dione (eq 2) were chosen as the models of unactive arenes and 1-(arylthio) pyrrolidine-2,5-diones used in experiment.[33] With the aid of DFT calculations, it is found that $Pd(TFA)_2(HOAc)_2$ should be considered as the active species, and the reaction proceeds in detail via C-H bond activation, concerted σ-bond metathesis, isomerization, ligand exchange, N-H protonation, and ligand exchange steps, differing from the mechanism proposed in experiment in which oxidative addition step is involved.[33] We expect our calculation results may help in understanding the mechanism of transition metal catalyzed C-S coupling reactions.

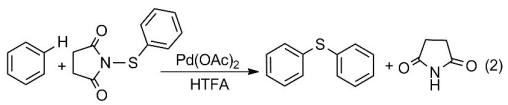

2. Computational Details

All geometry structures of reactants, products, intermediates, and transition states were

optimized by DFT calculations at the B3LYP level,[38] which has shown to be appropriate for the palladium catalyzed cross-coupling reactions.[39-42] The effective core potential (ECP) Stuttgart/Dresden triple-ζ SDD basis set[43] plus polarization functions (ζ_f=1.472)[44] was employed for Pd, while for all other main group atoms, the 6-31G** basis set was used. Frequency analyses were performed at the same level of theory to identify every stationary point as minimum (no imaginary frequencies) or transition state (only one imaginary frequency) and to provide the thermal correction to free energies at 298.15 K and 1 atm. Intrinsic reaction coordinates (IRC)[45] were calculated for all of the transition states to confirm that the structures indeed connect two relevant minima. Solvent effects were considered by performing single-point energy calculations for all the optimized structures at the M06 level[46] with a larger basis set 6-311+G** for all other main group atoms, using a continuum solvent model SMD.[47] This combination of employing B3LYP and M06 has been successfully applied in many transition-metal catalyzed C-H activation reactions, predicting the reaction mechanisms in good agreement with experimental observations.[48-52] Solvent HTFA was adopted with the self-defined solvent parameters using experiment determined dielectric constant of 8.55[53] and solvent radius of 2.479 Å.[54] In this paper, solvation- and entropy-corrected relative free energies are used to analyze the reaction mechanism. All of the calculations were performed with the Gaussian 09 software package.[55] The frontier molecular orbitals were drawn by Multiwfn[56] together with VMD.[57]

3. Result and Discussion

To determine the active species involved in the arylthiolation reaction, the thermodynamics of $Pd(OAc)_2$, $Pd(TFA)_2(HOAc)_2$,[58] $Pd(TFA)_2$, and $Pd(TFA)_2(HTFA)_2$ were analyzed as shown in Chart 1. It is found that $Pd(TFA)_2(HOAc)_2$ is the lowest one in energy among all of the palladium

complexes, suggesting that $Pd(TFA)_2(HOAc)_2$ is generated when $Pd(OAc)_2$ dissolved in HTFA. Therefore, in this paper, $Pd(TFA)_2(HOAc)_2$ was considered as active species to study the reaction mechanism.

Please insert Chart 1 here

In Scheme 2, two possible catalytic cycles I and II are presented. Catalytic cycle I involves two reaction pathways, one of which is oxidative addition pathway proposed in experiment.[33] First, the active species $Pd(TFA)_2(HOAc)_2$ reacts with benzene forming phenyl palladium(II) complex **A** via C-H bond activation. Oxidative addition of 1-(phenylthio) pyrrolidine-2,5-dione **R** to intermediate **A** gives a Pd(IV) intermediate **B** followed by reductive elimination to generate the arylthiolation product diaryl sulfide and intermediate **C**. Finally, protonation of **C** by HTFA completes the catalytic cycle I. In addition, the reaction of **A** with thiolating reagent **R** can occur directly through a σ-bond metathesis pathway to give palladium(II) complex **C** and diaryl sulfide. In catalytic cycle II, $Pd(TFA)_2(HOAc)_2$ reacts first with thiolating reagent **R**. Oxidative addition of **R** to $Pd(TFA)_2(HOAc)_2$ generates Pd(IV) intermediate **D**, then the C-H bond activation of benzene by **D** affords another Pd(IV) intermediate **B**, which is involved in catalytic cycle I.

Please insert Scheme 2 here

3.1 Catalytic cycle I

On the basis of catalytic cycle I depicted in Scheme 2, the Gibbs energy profiles for the arylthiolation reaction of benzene with 1-(phenylthio) pyrrolidine-2,5-dione **R** are illustrated in Fig. 1-5. From active species $Pd(TFA)_2(HOAc)_2$ **1**, there are two possible C-H activation pathways (Fig. 1). In one pathway, first, the replacement of HOAc molecule by benzene gives intermediate **2** having a C=C bond of benzene coordinated to metal center. Then, a concerted metalation-deprotonation

(CMD) process occurs via a six-membered transition state $\mathbf{TS_{2\text{-}3}}$ with an energy barrier of 22.3 kcal/mol relative to **1** to generate intermediate **3.** The CMD mechanism has been found in previous theoretical studies on Pd-catalyzed C-H bond activation reactions.[59-62] The other pathway first involves the dissociation of two HOAc molecules in active species **1** to form intermediate **1'**, which is higher in energy than **1** by 21.8 kcal/mol. Then, the C=C bond of benzene coordinates to **1'** giving intermediate **2'** followed by a CMD process to give intermediate **3'**. It is found that $\mathbf{TS_{2\text{-}3}}$ is lower in energy than $\mathbf{TS_{2'\text{-}3'}}$ by 12.0 kcal/mol, suggesting the reaction pathway $\mathbf{1 \rightarrow 2 \rightarrow TS_{2\text{-}3} \rightarrow 3}$ is more favorable in C-H activation process.

Please insert Fig. 1 here

From intermediate **3**, the replacement of HTFA molecule by thiolating substrate **R** gives two isomers **4** and **4'** (Fig. 2). The difference between **4** and **4'** is that the phenyl group on S is located above the palladium square plane in **4** while below the palladium plane in **4'**. As the reaction pathways from **4** and **4'** are similar, only the detailed pathways starting from **4** are presented in this paper while those starting from **4'** are depicted in Supporting Information. As shown in Fig. 2, from complex **4**, oxidative addition occurs through a three-membered transition state $\mathbf{TS_{4\text{-}5}}$ to give Pd(IV) intermediate **5**, which is 28.8 kcal/mol higher than **4**. Many theoretically studies have shown that Pd(IV) complex is thermodynamically unstable relative to Pd(II) complex in palladium catalyzed cross-coupling reactions.[54, 63, 64] From intermediate **4**, the reaction can also undergo a concerted σ-bond metathesis process through $\mathbf{TS_{4\text{-}6}}$ with the cleavage of the S-N and O-H bond as well as formation of the C-S and N-H bonds. Although $\mathbf{TS_{4\text{-}6}}$ is 8.9 kcal/mol lower than $\mathbf{TS_{4\text{-}5}}$, $\mathbf{TS_{4\text{-}6}}$ is still 34.5 kcal/mol relative to **1**, which is too high for the reactions occurring in 25°C. Therefore, besides those two pathways, other reaction mechanism should be considered.

Please insert Fig. 2 here

As shown in Fig. 3, dissociation of a HOAc molecule from intermediate **4** generates two complexes **7** (Fig. 3a) and **8** (Fig. 3b), respectively. In complex **7,** TFA ligand bonds to Pd center in an η^3 mode while in complex **8** one O atom of 1-(phenylthio) pyrrolidine-2,5-dione coordinates to Pd center. In Fig. 3a, oxidative addition of S-N bond occurs via a three-membered transition state $\mathbf{TS_{7\text{-}9}}$ giving the square pyramidal Pd(IV) complex **9**. Another pathway proceeds through σ-bond metathesis via transition state $\mathbf{TS_{7\text{-}10}}$ to form complex **10**. Transition state $\mathbf{TS_{7\text{-}10}}$ bears two three-membered rings having S bonded to Pd with Pd-S bond of 2.294 Å. The transition states $\mathbf{TS_{7\text{-}9}}$ and $\mathbf{TS_{7\text{-}10}}$ are as high as 46.6 and 42.5 kcal/mol reactive to **1**, respectively, suggesting the reaction is kinetically unfavorable. From complex **8** (Fig. 3b), oxidative addition process occurs via a three-membered transition state $\mathbf{TS_{8\text{-}11}}$ to generate the octahedral Pd(IV) complex **11**. The σ-bond metathesis process is also considered**,** but the corresponding transition state having two three-membered rings was not located. Instead, an interesting concerted σ-bond metathesis transition state $\mathbf{TS_{8\text{-}12}}$ was found, in which one O of 1-(phenylthio) pyrrolidine-2,5-dione bonds to Pd center. $\mathbf{TS_{8\text{-}12}}$ has one three-membered and one five-membered rings with Pd-S bond of 2.188 Å. The S-N bond is only 0.336 Å lengthened in $\mathbf{TS_{8\text{-}12}}$ (2.097 Å) compared to that in complex **8** (1.761 Å), giving $\mathbf{TS_{8\text{-}12}}$ just 23.6 kcal/mol higher than **8**. Comparing the six pathways shown in Fig. 2 and 3, $\mathbf{TS_{8\text{-}12}}$ is the lowest one with an energy barrier of 24.3 kcal/mol relative to **1**, indicating that the pathway **4→8→**$\mathbf{TS_{8\text{-}12}}$**→12** involved in concerted σ-bond metathesis mechanism is more favorable than the pathway **4→8→**$\mathbf{TS_{8\text{-}11}}$**→11** involved in oxidative addition mechanism for the cleavage of S-N bond.

Please insert Fig. 3 here

From complex **12**, two isomerization reaction pathways have been found and shown in Fig. 4.

In one isomerization pathway, the reaction is initiated by ligand exchange of O atom in TFA ligand for phenyl C=C bond in diaryl sulfide to produce intermediate **13**, followed by replacement of O atom with N atom via transition state $\mathbf{TS_{13\text{-}14}}$ generating complex **14**. The other isomerization pathway occurs via transition state $\mathbf{TS_{12\text{-}14}}$ by replacement of O atom with N atom to produce directly complex **14**, which contains a chelate trifluoroacetate ligand. IRC calculation for $\mathbf{TS_{12\text{-}14}}$ has verified that the structure indeed connects complex **12** and **14** as two relevant minima (see the Fig. S1 in Supporting information). From Fig. 4, $\mathbf{TS_{12\text{-}14}}$ is lower than $\mathbf{TS_{13\text{-}14}}$ by 4.1 kcal/mol, suggesting the pathway **12**→$\mathbf{TS_{12\text{-}14}}$→**14** is preferred.

Please insert Fig. 4 here

The energy profile for the regeneration of active species **1** from **14** has been shown in Fig. 5. From **14**, the ligand exchange of diaryl sulfide by HTFA occurs through transition state $\mathbf{TS_{14\text{-}15}}$ to release product diaryl sulfide and form intermediate **15**. Complex **15** contains a weak non-covalent interaction with a hydrogen bond of 1.62 Å between H and N atoms. Subsequently, N-H protonation process occurs through transition state $\mathbf{TS_{15\text{-}16}}$ giving complex **16,** having a hydrogen bond of 1.58 Å between H and O atoms. From intermediate **16**, coordination of HOAc and releasing of pyrrolidine-2,5-dione forms complex **17**. Finally, coordination of HOAc regenerates the active species **1**.

Please insert Fig. 5 here

3.2 Catalytic cycle II

The reaction of active species $Pd(TFA)_2(HOAc)_2$ **1** with thiolating substrate **R** is shown in Fig. 6. The replacement of one HOAc molecule by **R** gives intermediate **18.** Subsequent oxidative addition of S-N bond to intermediate **18** proceeds via transition state $\mathbf{TS_{18\text{-}19}}$ to form an octahedral Pd(IV)

complex **19.** In addition, dissociation of two HOAc molecules from **1** generates intermediate **1'**. Then thiolating reagent **R** coordinates to **1**' giving intermediate **20**, from which oxidative addition process occurs via transition state $\mathbf{TS_{20\text{-}21}}$ to form another octahedral Pd(IV) complex **21**. Both two reaction pathways are kinetically unfavorable because of the high energy barriers of more than 49 kcal/mol. Therefore, catalytic cycle I is preferred to catalytic cycle II for the arylthiolation reaction.

Please insert Fig. 6 here

3.3 Reaction mechanism of arylthiolation reaction

Based on the overall reaction pathways involved in catalytic cycles I and II, the energy profile of the most favorable pathway is shown in Fig. 7. The arylthiolation reaction of benzene with 1-(phenylthio) pyrrolidine-2,5-dione to form diaryl sulfide occurs via C-H bond activation, concerted σ-bond metathesis, isomerization, ligand exchange, N-H protonation, and ligand exchange steps. The concerted σ-bond metathesis is found to be the rate-determining step in this reaction process. The overall activation barrier ($\mathbf{TS_{8\text{-}12}}$) for rate-determining step is 24.3 kcal/mol, in consistent with the mild experimental reaction condition (25°C).[33] However, the concerted σ-bond metathesis mechanism is different from the oxidative addition mechanism proposed by experiment.[33] Here we compared the structures of intermediate **8**, transition states $\mathbf{TS_{8\text{-}11}}$ and $\mathbf{TS_{8\text{-}12}}$ involved in Fig. 3 (as shown in Fig. 8). It is found that the S-N bond (2.097 Å) and Pd-S-N angle (88.0°) in $\mathbf{TS_{8\text{-}12}}$ are only 0.336 Å lengthened and only 8.5° strained relative to these (1.761 Å of S-N bond and 96.5° of Pd-S-N angle) in intermediate **8,** respectively, while in $\mathbf{TS_{8\text{-}11}}$ the S-N bond (2.432 Å) and Pd-S-N angle (57.1°) are 0.671 Å lengthened and 39.4° strained, respectively. The relatively small structural changes in concerted σ-bond metathesis transition state $\mathbf{TS_{8\text{-}12}}$ give it lower than the oxidative addition transition state $\mathbf{TS_{8\text{-}11}}$ in energy.

Please insert Fig. 7 here

Please insert Fig. 8 here

In order to probe the nature of the difference between the theoretical and experimental reaction mechanism, we analyzed the frontier molecular orbitals for intermediate **8.** The two highest occupied molecular orbitals (HOMO and HOMO-1) and the lowest unoccupied molecular orbital (LUMO) of intermediate **8** were presented in Fig. 9. As shown in Fig. 9a, the HOMO mainly corresponds to the π bonding orbital of the phenyl ligand (74%) and HOMO-1 mainly consists of the Pd occupied d orbital (53%), while the LUMO is composed of a major contribution of the σ* anti-bonding of the S-N bond (46%). The concerted σ-bond metathesis mechanism involves the cleavage of the S-N and Pd-C bonds as well as the formation of the C-S bond. It is seen that this step from intermediate 8 (see Fig. 3) is best activated through the HOMO-LUMO interaction, i.e., the π bonding orbital of phenyl donates π electrons to σ* orbital of the S-N bond. Meanwhile, on the basis of the orbital analysis of these frontier molecular orbitals, one can envisage the electron flow during this process, which is presented in Fig. 9b. In the concerted σ-bond metathesis transition state $\mathbf{TS_{8\text{-}12}}$, the electron pair on the π bonding orbital of phenyl transfers to S, the S-N bond electrons to N center, lone pair electrons on N to C, C=O π electrons to O center, O lone pair electrons to Pd, and the Pd-C bond electrons to C leading to the formation of intermediate **12**. On the other hand, the oxidative addition mechanism involves the S-N bond cleavage and the formation of the Pd-S and Pd-N bonds (Fig. 3), which is activated through the orbital interaction between the HOMO-1 and LUMO, i.e., σ-donation of Pd 4d electrons to σ*(S-N). In the oxidative addition transition state $\mathbf{TS_{8\text{-}11}}$, the electron pair on the Pd d orbital moves to N atom forming the Pd-N bond, the S-N bond electrons to S center, resulting in the cleavage of the S-N bond, and the lone pair electrons on S to Pd giving the Pd-S bond (Fig. 9b). On

the basis of the orbital analysis mentioned above, it is clear that the concerted σ-bond metathesis mechanism (via **$TS_{8\text{-}12}$**) is much more favored when compared with the oxidative addition mechanism (via **$TS_{8\text{-}11}$**).

Please insert Fig. 9 here

Conclusion

The reaction mechanism of palladium catalyzed arylthiolation of benzene with 1-(phenylthio) pyrrolidine-2,5-dione to form diaryl sulfide has been theoretically investigated by utilizing DFT calculations. The calculations indicate that $Pd(TFA)_2(HOAc)_2$ should be considered as active species since $Pd(TFA)_2(HOAc)_2$ is the lowest one in energy among $Pd(OAc)_2$, $Pd(TFA)_2(HOAc)_2$, $Pd(TFA)_2$, and $Pd(TFA)_2(HTFA)_2$. Two catalytic cycles (I and II) have been taken into account. It is found that catalytic cycle I is more preferred, which involves C-H bond activation, concerted σ-bond metathesis, isomerization, ligand exchange, N-H protonation, and ligand exchange steps. The present reaction mechanism is slightly different from the one proposed by Anbarasan et al. in experiment,[33] which includes oxidative addition of the S-N bond. The relatively small structural changes in concerted σ-bond metathesis transition state compared to the oxidative addition one give the former lower than the latter in energy. In addition, frontier molecular orbitals were further analyzed to understand the nature of different reaction mechanism between concerted σ-bond metathesis and oxidative addition. The results suggest that HOMO-LUMO interaction (π-donation of phenyl to σ*(S-N)) gives concerted σ-bond metathesis while interaction between the HOMO-1 and LUMO (σ-donation of Pd 4d electrons to σ*(S-N)) results in the oxidative addition, and thus, the concerted σ-bond metathesis is preferred to oxidative addition in the arylthiolation reaction.

Supporting Information Available. Text giving IRC calculation of $\mathbf{TS_{12\text{-}14}}$, comparison of reactions of complex **14** with HTFA and HOAc, reaction pathways from intermediate **4'**, Cartesian coordinates for all of the calculated structures. This information is available free of charge via the internet at http://pubs.rsc.org.

Corresponding Authors

*E-mail for J.L.: ljy121@jlu.edu.cn.

*E-mail for M.W.: mywang858@163.com.

Notes

The authors declare no competing financial interest.

Acknowledgments. This work was supported by the National Natural Science Foundation of China (Grants 21373098 and 21203073). The authors are grateful to Computing Center of Jilin Province for essential support.

References

1. G. Liu, J. R. Huth, E. T. Olejniczak, R. Mendoza, P. DeVries, S. Leitza, E. B. Reilly, G. F. Okasinski, S. W. Fesik and T. W. von Geldern, *J. Med. Chem.*, 2001, **44**, 1202-1210.

2. M. L. Alcaraz, S. Atkinson, P. Cornwall, A. C. Foster, D. M. Gill, L. A. Humphries, P. S. Keegan, R. Kemp, E. Merifield, R. A. Nixon, A. J. Noble, D. O'Beirne, Z. M. Patel, J. Perkins, P. Rowan, P. Sadler, J. T. Singleton, J. Tornos, A. J. Watts and I. A. Woodland, *Org. Process Rev. Dev.*, 2005, **9**, 555-569.

3. S. Pasquini, C. Mugnaini, C. Tintori, M. Botta, A. Trejos, R. K. Arvela, M. Larhed, M. Witvrouw, M. Michiels, F. Christ, Z. Debyser and F. Corelli, *J. Med. Chem.*, 2008, **51**, 5125-5129.

4. S. Raghavan, V. Krishnaiah and B. Sridhar, *J. Org. Chem.*, 2010, **75**, 498-501.

5. E. A. Ilardi, E. Vitaku and J. T. Njardarson, *J. Med. Chem.*, 2014, **57**, 2832-2842.

6. C. C. Eichman and J. P. Stambuli, *Molecules*, 2011, **16**, 590-608.

7. T. Migita, T. Shmizu, Y. Asami, J. Shiobara, Y. Kato and M. Kosugi, *Bull. Chem. Soc. Jpn.*, 1980, **53**, 1385-1389.

8. E. Alvaro and J. F. Hartwig, *J. Am. Chem. Soc.*, 2009, **131**, 7858-7868.

9. P. S. Herradura, K. A. Pendola and R. K. Guy, *Org. Lett.*, 2000, **2**, 2019-2022.

10. C. Palomo, M. Oiarbide, R. Lopez and E. Gomez-Bengoa, *Tetrahedron Lett.*, 2000, **41**, 1283-1286.

11. X. B. Xu, J. Liu, J. J. Zhang, Y. W. Wang and Y. Peng, *Org. Lett.*, 2013, **15**, 550-553.

12. H. Wang, L. Wang, J. Shang, X. Li, H. Wang, J. Gui and A. Lei, *Chem. Commun.*, 2012, **48**, 76-78.

13. V. P. Reddy, K. Swapna, A. V. Kumar and K. R. Rao, *J. Org. Chem.*, 2009, **74**, 3189-3191.

14. C. F. Lee, Y. C. Liu and S. S. Badsara, *Chem. -Asian. J.*, 2014, **9**, 706-722.

15. C. Shen, P. Zhang, Q. Sun, S. Bai, T. S. Hor and X. Liu, *Chem. Soc. Rev.*, 2015, **44**, 291-314.

16. S. Zhang, P. Qian, M. Zhang, M. Hu and J. Cheng, *J. Org. Chem.*, 2010, **75**, 6732-6735.

17. J. H. Cheng, C. L. Yi, T. J. Liu and C. F. Lee, *Chem. Commun.*, 2012, **48**, 8440-8442.

18. P. Anbarasan, H. Neumann and M. Beller, *Chem. Commun.*, 2011, **47**, 3233-3235.

19. C. Yu, C. Zhang and X. Shi, *Eur. J. Org. Chem.*, 2012, **2012**, 1953-1959.

20. X. Chen, X. S. Hao, C. E. Goodhue and J. Q. Yu, *J. Am. Chem. Soc.*, 2006, **128**, 6790-6791.

21. L. Chu, X. Yue and F. L. Qing, *Org. Lett.*, 2010, **12**, 1644-1647.

22. M. Iwasaki, M. Iyanaga, Y. Tsuchiya, Y. Nishimura, W. J. Li, Z. P. Li and Y. Nishihara, *Chem.-*

Eur. J., 2014, **20**, 2459-2462.

23. C. Lin, D. Li, B. Wang, J. Yao and Y. Zhang, *Org. Lett.*, 2015, **17**, 1328-1331.

24. S. Y. Yan, Y. J. Liu, B. Liu, Y. H. Liu and B. F. Shi, *Chem. Commun.*, 2015, **51**, 4069-4072.

25. V. P. Reddy, R. Qiu, T. Iwasaki and N. Kambe, *Org. Biomol. Chem.*, 2015, **13**, 6803-6813.

26. S. Ranjit, R. Lee, D. Heryadi, C. Shen, J. Wu, P. Zhang, K. W. Huang and X. Liu, *J. Org. Chem.*, 2011, **76**, 8999-9007.

27. C. Dai, Z. Xu, F. Huang, Z. Yu and Y. F. Gao, *J. Org. Chem.*, 2012, **77**, 4414-4419.

28. S.-i. Fukuzawa, E. Shimizu, Y. Atsuumi, M. Haga and K. Ogata, *Tetrahedron Lett.*, 2009, **50**, 2374-2376.

29. D. Alves, R. G. Lara, M. E. Contreira, C. S. Radatz, L. F. B. Duarte and G. Perin, *Tetrahedron Lett.*, 2012, **53**, 3364-3368.

30. M. Chen, Z. T. Huang and Q. Y. Zheng, *Chem. Commun.*, 2012, **48**, 11686-11688.

31. H. Tian, H. Yang, C. Zhu and H. Fu, *Adv. Synth. Catal.*, 2015, **357**, 481-488.

32. C. Zhang, J. McClure and C. J. Chou, *J. Org. Chem.*, 2015, **80**, 4919-4927.

33. P. Saravanan and P. Anbarasan, *Org. Lett.*, 2014, **16**, 848-851.

34. A. Milet, A. Dedieu, G. Kapteijn and G. V. Koten, *Inorg. Chem.*, 1997, **36**, 3223-3231.

35. K. C. Lam, T. B. Marder and Z. Y. Lin, *Organometallics*, 2010, **29**, 1849-1857.

36. N. Kirai, J. Takaya and N. Iwasawa, *J. Am. Chem. Soc.*, 2013, **135**, 2493-2496.

37. O. Swang, R. Blom and B. O. Ryan, *J. Phys. Chem.*, 1996, **100**, 17334-17336.

38. A. D. Becke, *J. Chem. Phys.*, 1993, **98**, 5648.

39. H. J. Xie, F. R. Lin, Q. F. Lei and W. J. Fang, *Organometallics*, 2013, **32**, 6957-6968.

40. Y. F. Dang, S. L. Qu, Z. X. Wang and X. T. Wane, *J. Am. Chem. Soc.*, 2014, **136**, 986-998.

41. S. L. Zhang, Y. Fu, R. Shang, Q. X. Guo and L. Liu, *J. Am. Chem. Soc.*, 2010, **132**, 638-646.

42. J. L. Jiang, J. Q. Yu and K. Morokuma, *ACS Catal.*, 2015, **5**, 3648-3661.

43. M. Dolg, U. Wedig, H. Stoll and H. Preuss, *J. Chem. Phys.*, 1987, **86**, 866.

44. A. Ariafard, E. S. Tabatabaie, A. T. Monfared, S. H. A. Assar, C. J. T. Hyland and B. F. Yates, *Organometallics*, 2012, **31**, 1680-1687.

45. K. Fukui, *J. Phys. Chem.*, 1970, **74**, 4161-4163.

46. Y. Zhao and D. G. Truhlar, *Theor. Chem. Acc.*, 2008, **120**, 215-241.

47. A. V. Marenich, C. J. Cramer and D. G. Truhlar, *J. Phys. Chem. B.*, 2009, **113**, 6378-6396.

48. J. S. Cannon, L. F. Zou, P. Liu, Y. Lan, D. J. O'Leary, K. N. Houk and R. H. Grubbs, *J. Am. Chem. Soc.*, 2014, **136**, 6733-6743.

49. R. Giri, Y. Lan, P. Liu, K. N. Houk and J. Q. Yu, *J. Am. Chem. Soc.*, 2012, **134**, 14118-14126.

50. Q. Xie, X. S. Song, D. Qu, L. P. Guo and Z. Z. Xie, *Organometallics*, 2015, **34**, 3112-3119.

51. A. J. Canty, A. Ariafard, B. F. Yates and M. S. Sanford, *Organometallics*, 2015, **34**, 1085-1090.

52. Q. Zhang, H. Z. Yu and Y. Fu, *Organometallics*, 2013, **32**, 4165-4173.

53. F. E. Harris and C. T. OKonski, *J. Am. Chem. Soc.*, 1954, **76**, 4317-4318.

54. D. Munz, D. Meyer and T. Strassner, *Organometallics*, 2013, **32**, 3469-3480.

55. Frisch, M. J. In *Gaussian 09*, *revision A.02*; Gaussian, Inc., Wallingford, CT, 2009

56. T. Lu and F. W. Chen, *J. Comput. Chem.*, 2012, **33**, 580-592.

57. W. Humphrey, A. Dalke and K. Schulten, *J. Mol. Graph.*, 1996, **14**, 33-38, 27-38.

58. $Pd(OAc)_2$ dissloved in HTFA by coordination of two HTFA molecules to palladium center, forming $Pd(OAc)_2(HTFA)_2$, but $Pd(OAc)_2(HTFA)_2$ can't be located. It is extremely stable that it directly form $Pd(TFA)_2(HOAc)_2$.

59. S. Rousseaux, S. I. Gorelsky, B. K. W. Chung and K. Fagnou, *J. Am. Chem. Soc.*, 2010, **132**, 10692-10705.

60. H. Y. Sun, S. I. Gorelsky, D. R. Stuart, L. C. Campeau and K. Fagnou, *J. Org. Chem.*, 2010, **75**, 8180-8189.

61. D. E. Stephens, J. Lakey-Beitia, A. C. Atesin, T. A. Atesin, G. Chavez, H. D. Arman and O. V. Larionov, *ACS Catal.*, 2015, **5**, 167-175.

62. S. I. Gorelsky, *Organometallics*, 2012, **31**, 4631-4634.

63. Z. F. Ke and T. R. Cundari, *Organometallics*, 2010, **29**, 821-834.

64. Y. Wei, H. R. Tang, X. F. Cong, B. Bin Rao, C. Wu and X. M. Zeng, *Org. Lett.*, 2014, **16**, 2248-2251.

Figure captions

Chart 1. Thermodynamics of $Pd(OAc)_2$, $Pd(TFA)_2(HOAc)_2$, $Pd(TFA)_2$, and $Pd(TFA)_2(HTFA)_2$. The calculated relative free energies are given in kcal/mol.

Scheme 1. Possible catalytic cycle proposed by Anbarasan *et al.* in ref 33.

Scheme 2. Proposed catalytic cycles for palladium catalyzed direct arylthiolation of benzene to 1-(phenylthio) pyrrolidine-2,5-dione.

Fig. 1. Gibbs energy profiles calculated for the reaction of active species **1** with benzene through concerted metalation-deprotonation (CMD) mechanism to form Pd(II) intermediate **3** and **3'**. The calculated relative free energies are given in kcal/mol.

Fig. 2. Gibbs energy profiles calculated for oxidative addition and concerted σ-bond metathesis giving intermediates **5** and **6**. The calculated relative free energies are given in kcal/mol.

Fig. 3. Gibbs energy profiles calculated for oxidative addition and σ-bond metathesis giving intermediates **9**, **10**, **11**, and **12**. The calculated relative free energies are given in kcal/mol.

Fig. 4. Gibbs energy profiles calculated for the isomerization reaction from **12** to **14**. The calculated relative free energies are given in kcal/mol.

Fig. 5. Gibbs energy profile calculated for the regeneration of active species **1** from intermediate **14**. The calculated relative free energies are given in kcal/mol.

Fig. 6. Gibbs energy profiles calculated for the reaction of active catalyst **1** with thiolating substrate **R**. The calculated relative free energies are given in kcal/mol.

Fig. 7. The overall Gibbs energy profile calculated for the palladium catalyzed arylthiolation reaction of benzene with 1-(phenylthio) pyrrolidine-2,5-dione. The calculated relative free energies are given in kcal/mol.

Fig. 8. Geometry structures with selected parameters for intermediate **8** and transition state $\mathbf{TS_{8\text{-}11}}$ and $\mathbf{TS_{8\text{-}12}}$. The bond lengths and bond angles are given in angstroms and degrees, respectively.

Fig. 9. (a) HOMO-1, HOMO and LUMO of intermediate **8**; (b) Orbital interactions and electron transfers in oxidative addition transition state $\mathbf{TS_{8\text{-}11}}$ and concerted σ-bond metathesis transition state $\mathbf{TS_{8\text{-}12}}$.

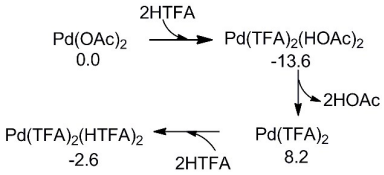

Chart 1

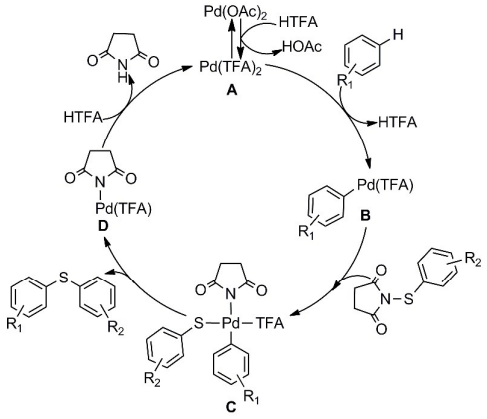

Scheme 1

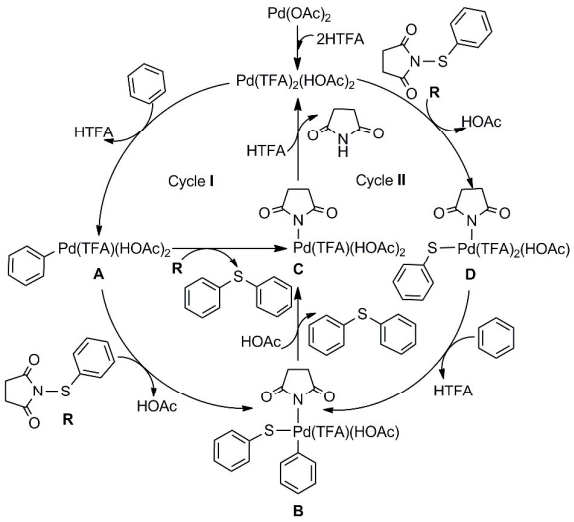

Scheme 2

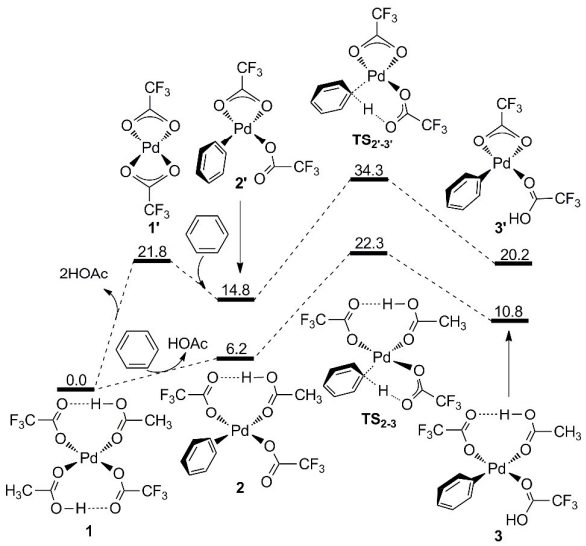

Fig. 1

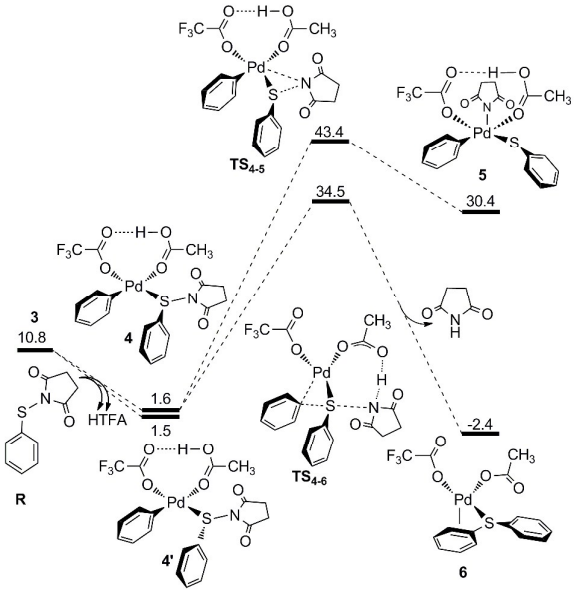

Fig. 2

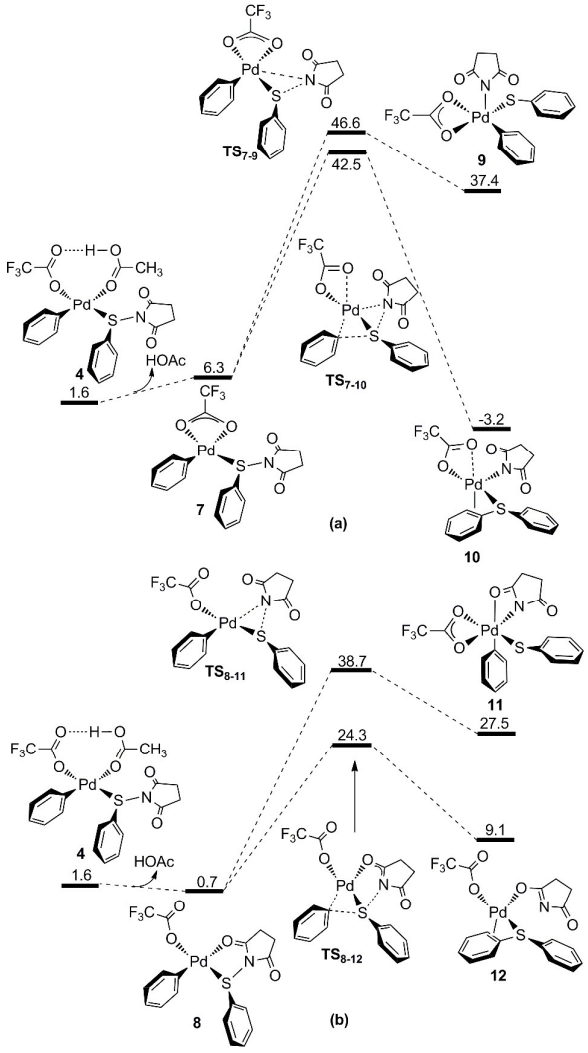

Fig. 3

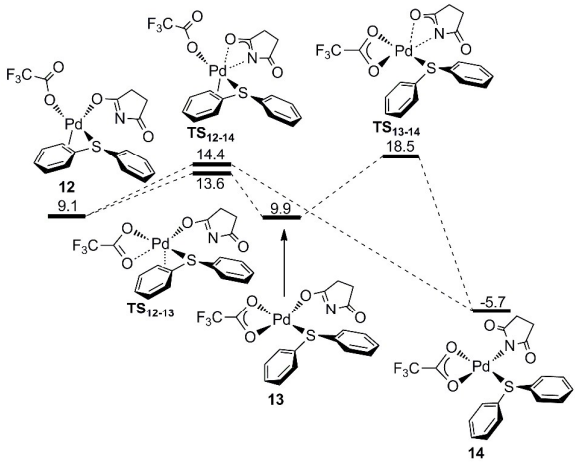

Fig. 4

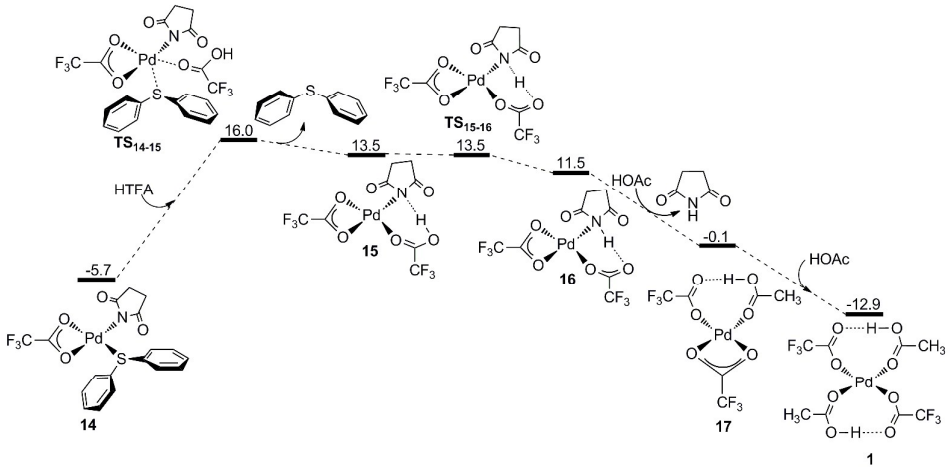

Fig. 5

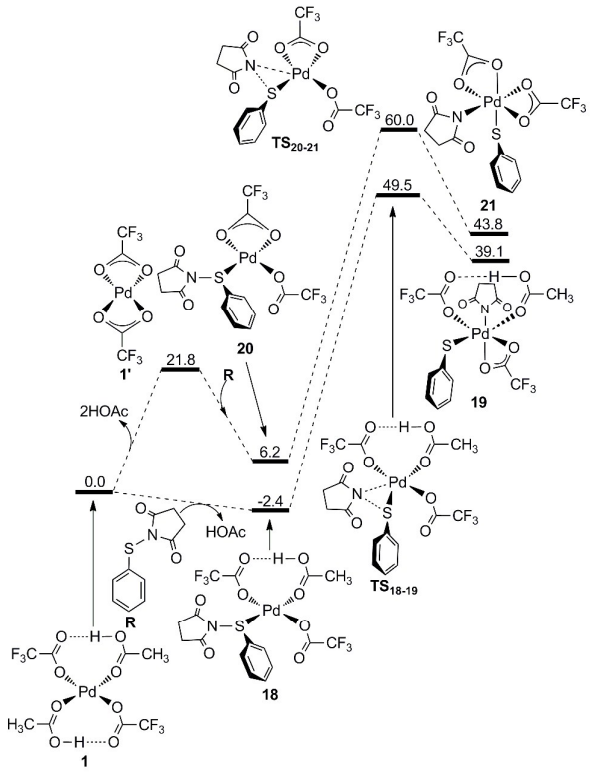

Fig. 6

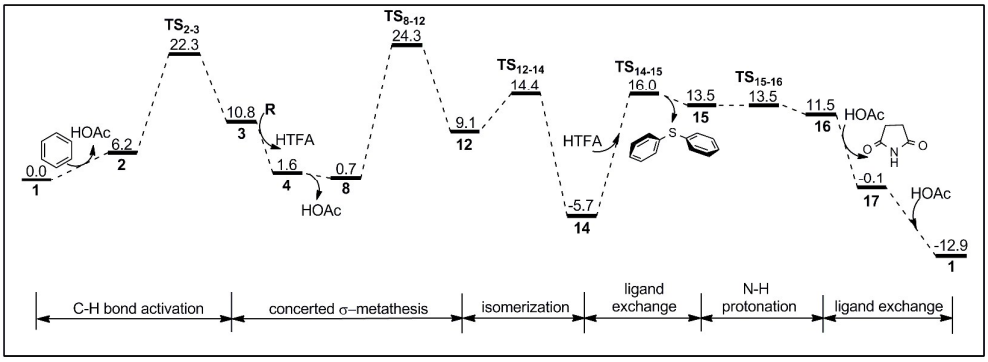

Fig. 7

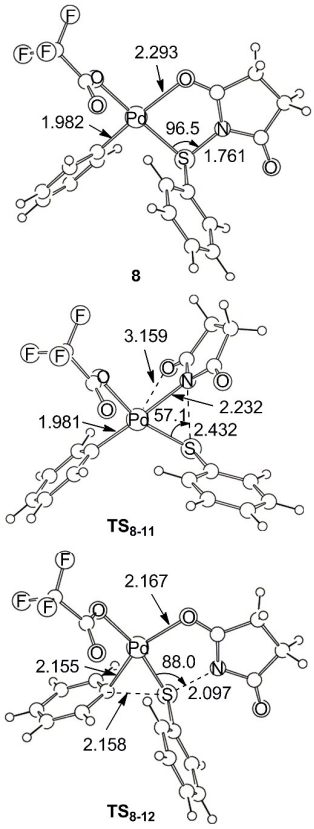

Fig. 8

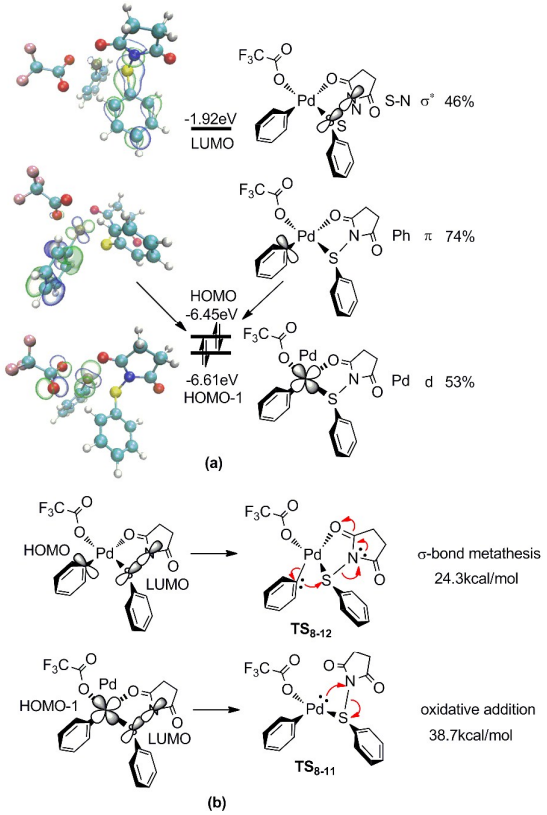

Fig. 9

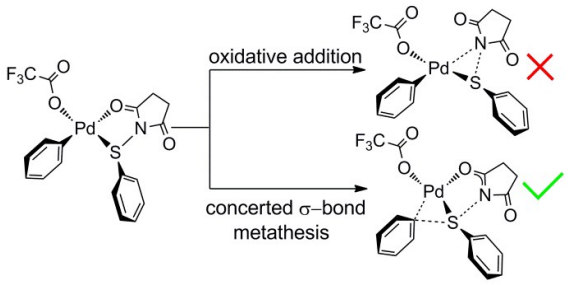

TOC

The cleavage of S-N bond prefers to take place via concerted σ-bond metathesis rather than oxidative addition proposed in experiment.